Floquet-Bloch theory of high-harmonic generation in periodic structures

F. H. M. Faisal
Fakultät für Physik, Universität Bielefeld, 33 615 Bielefeld 1, Germany

J. Z. Kamiński
Institute of Theoretical Physics, Warsaw University, Hoża 69, 00-681 Warszawa, Poland

(Received 12 February 1997)

Generation of high harmonics by the interaction of intense laser fields with periodic crystal structures is investigated theoretically. A nonperturbative Floquet-Bloch theory of the interacting system (crystal plus laser field) is developed and applied to obtain the field-modified band structure of the system. The mean energy spectrum, the dispersion and the fluctuation of the band energy in the photon space, and the associated standard deviation and spectral entropy are calculated. The harmonic generation spectra in a thin crystal, for the neodymium-doped yttrium aluminum garnet laser frequency $\omega = 1.169$ eV, are obtained, both in the perturbative and nonperturbative intensity domains. The calculated emission spectra for an insulator, a semiconductor, and a metal film are compared. The semiconductor medium is found to be somewhat more efficient than the metal or the insulator. A ''transition intensity'' for strong harmonic generation in crystalline media occurs at about an intensity $I = 10^{-4}$ a.u., i.e., 3.51×10^{12} W/cm^2. [S1050-2947(97)06007-1]

PACS number(s): 42.50.Hz, 42.65.Ky, 32.80.Wr

I. INTRODUCTION

The earliest experiments on the generation of harmonics in intense laser fields showed the formation of a plateau in the energy distribution of the coherently emitted harmonics up to a high order [1]. Because of its clear nonperturbative character, this finding stimulated much interest, both from experimental [2] and theoretical [3] points of view. In these experiments noble gas atoms were predominantly used as the ''active media.'' Recently a number of experiments were carried out in the intensity range between 10^9 and 10^{17} W/cm^2, giving rise to high-harmonic generation from solid targets [4,5].

Theoretical studies of high-harmonic generation in condensed-matter media have also been initiated recently [6–10]. The purpose of this paper is to present a microscopic Floquet-Bloch theory of nonperturbative interaction of intense laser light with periodic structures, and apply it to the problem of modification of the band structure by the field and the generation of high harmonics in such media.

Before proceeding further, we qualitatively estimate a number of macroscopic parameters relevant for practical realization purposes. The skin-depth of electromagnetic radiation say, at the wavelength of neodymium-doped yttrium aluminum garnet (Nd:YAG) laser ($\lambda = 1064$ nm) for a metallic crystal (electron density 10^{23}/cm^3) is about 170 Å. We may thus assume a typical width of the thin metallic crystal or film (especially in the perpendicular incidence mode) to be of the order of 100 Å. For a grazing incidence of the light beam, this will permit field interaction with the crystal electrons over the entire width. For an intrinsic semiconductor target, the carrier density being much smaller (e.g., Ge: 2×10^{13}/cm^3), the skin depth is much greater, and the limit on the width may be considerably extended. Unlike in the gaseous media, the laser intensity might not be increased indefinitely, or the laser pulse duration may not be too long, in solid media due to possible damage to the crystal. Note that for an atomic layer of moderate Z materials of 100 Å, in the field of a Nd:YAG laser of 10^{15} W/cm^2, the lattice disintegration time has been estimated to be several hundred fs [7], and the electron-phonon relaxation time [11] to be a few hundred fs. One may thus allow an intensity as high as 10^{15} W/cm^2 for a Nd:YAG laser pulse of 100 fs, without thermally damaging the lattice. But perhaps a more severe restriction on the intensity of the field is imposed by the characteristic intensity for the ionization breakdown of the crystal. There are at present no definitive estimates of this available . However, we may obtain an order of magnitude estimate for this purpose by assuming it to be about the threshold intensity for the onset of the ATI (above threshold ionization) process. The ATI threshold generally occurs for $U_p > \hbar\omega$, where U_p is the so-called ponderomotive energy. For the Nd:YAG laser this gives an intensity of the order of 10^{13} W/cm^2. We shall therefore restrict ourselves to intensities below this value for the numerical applications of the theory in the present work. The above expectations on the limiting pulse durations and intensities are also found to be consistent with the recent experiments using a 35 ps pulsed Nd:YAG laser at an intensity of 5 GW/cm^2 on gold targets [4] and a 170 fs pulsed Ti:sapphire laser at an intensity of 10^{17}W/cm^2 [5] on aluminum targets. Long nanosecond laser pulses [12], on the other hand, are not suitable for the purpose. Propagation of the fundamental and generated harmonics in the crystal (especially in the perpendicular incidence mode) may also lead to a possible loss of phase coherence. However, this problem need not be too severe for propagation within the 100 Å width, but could set a limit on the highest coherent harmonic to be generated. A recently proposed technique of ''quasi-phase-matching'' [13,14], using suitably fabricated periodically segmented structures of different indices [15], could also help to relax this restriction. Moreover, with suitably constructed periodic structures, such techniques may even lead to a possible selection of a given harmonic from the generated spectrum, by quasi-phase-

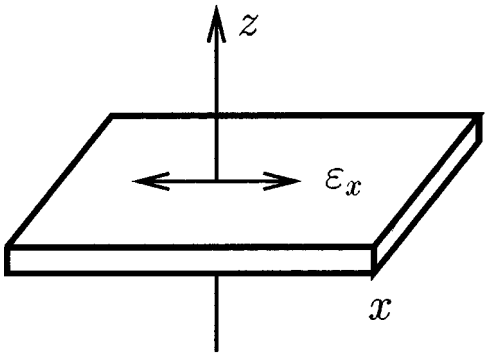

FIG. 1. Schematic of a possible geometric arrangement of the crystal and the field for high harmonic generation.

matching the selected harmonic with the fundamental. Keeping the above laboratory restrictions and prospects in mind, we turn now to the formulation of a nonperturbative microscopic theory of interaction of intense laser fields with an idealized periodic crystal.

II. THEORETICAL FORMULATION

In Fig. 1 we show a schematic of a perpendicular incidence geometry for high-harmonic generation in thin films. In this mode the laser pulse is assumed to cross the film from below upward (z axis), and is taken to be polarized along the x axis; the emitted harmonics are expected predominantly to emerge in the direction of the propagation of the field. We note already that unlike in the grazing-incidence geometry, where due to the absence of the inversion symmetry both odd and even harmonics are generated, in the perpendicular incidence geometry, due to the presence of the inversion symmetry, only odd harmonics are permitted.

To obtain detailed insights into the field-induced processes in solids, e.g. modification of the band strcture, resonant interband transitions, dependence of the harmonic signal on induced currents, Bloch vectors, or band filling, we develop a Floquet-Bloch theory of the interaction of a crystal with a monochromatic laser field. The field is also supposed to be switched on and off adiabatically, and thus to have a typical pulse duration much greater than the field oscillation period. As usual, the dipole approximation for the laser field, that is generally well justified for infrared and optical frequencies [16], will be assumed. The crystal electrons are assumed to move independently in a static background field of the ions forming the lattice, where the background field can be approximated by a periodic model potential (e.g., [17]). The motion of the lattice electrons is assumed to be along the direction of the polarization of the field, and hence is quasi-one-dimensional in nature. Thus the theory developed below can be equally well applied to the investigations of laser interaction with artificial one-dimensional semiconductor heterostructures [18], that can nowadays be fabricated in the laboratory.

An exactly soluble model

In order to discuss a number of general properties of nonperturbative interactions of electrons in a crystal lattice with an intense laser field, in this section we consider an exactly soluble model. This model is defined by the time-dependent Schödinger equation (we use units in which $\hbar=1$)

$$i\partial_t\Psi(x,t)=\left[-\frac{1}{2\mu}\frac{\partial^2}{\partial x^2}+\frac{P}{2a}\sum_{m\in\mathcal{Z}}\delta(x-ma)+\frac{ie}{\mu c}A(t)\frac{\partial}{\partial x}+\frac{e^2}{2\mu c^2}A^2(t)\right]\Psi(x,t), \tag{1}$$

where $\mathcal{Z}$ stands for all integers positive, negative, and zero. In the above the lattice potential is chosen to be the well-known Kronig-Penney periodic δ potentials of strength $P/2a$, with the lattice constant a [19]. The laser field is assumed to be linearly polarized along the crystal axis in the x direction, and is given by the vector potential

$$A(t)=A_0\cos(\omega t+\delta), \tag{2}$$

where A_0 is related to the peak field strength of the laser F_0, $F_0=(\omega/c)A_0$, ω is the frequency, and δ is an arbitrary phase.

This model has been initially studied by Tsoar and Gersten [20], who obtained the dispersion relation of the system in terms of a double-infinite matrix, and discussed the modification of the band structure with approximate calculations. It was shown afterwards [21,22] how to obtain an exact analytic solution of the dispersion relation of the system in terms of a single-infinite matrix. This greatly facilitates both an exact calculation of the band structure and a discussion of general features of such systems when the laser field can no longer be treated by the perturbation theory.

It is useful to introduce a phase transformation of the wave function,

$$\Psi(x,t)=\exp\left[-\frac{ie^2}{2\mu c^2}\int^t dt' A^2(t')\right]\psi(x,t), \tag{3}$$

and work with $\psi(x,t)$, which now satisfies the same Schrödinger equation (1) but without the last $A^2(t)$ term.

We note that the Hamiltonian is periodic both in space and time dimensions. The time-periodic property is given by the Floquet theorem, and the space-periodic property is given by the Bloch theorem (the latter being merely a spatial analog of the former). Thus we first apply the Floquet-Fourier expansion (e.g., [23])

$$\psi(x,t)=e^{-iEt}\sum_{n\in\mathcal{Z}}e^{-in(\omega t+\delta)}\psi_n(x), \tag{4}$$

where E is in general noncomensurate with ω and represents a so-called quasienergy. Substitution of Eq. (4) into Eq. (1) leads to the Floquet-Schrödinger equation for the Floquet-Fourier components $\psi_n(x)$,

$$(E-H_n)\psi_n(x)=0, \quad n=0,\pm1,\pm2,\ldots, \tag{5}$$

where the Floquet Hamiltonian is given by

$$H_n=-\frac{1}{2\mu}\frac{\partial^2}{\partial x^2}+\frac{P}{2a}\sum_{m\in\mathcal{Z}}\delta(x-ma)$$
$$+\frac{1}{2}i\omega\alpha_0(S_n^+-S_n^-)\frac{\partial}{\partial x}-n\omega. \quad (6)$$

In the above equation the so-called index-shift operators $S_n^{\pm}$ merely shift the index n of ψ_n,

$$S_n^{\pm}\psi_n(x)=\psi_{n\pm1}(x), \quad (7)$$

and the constant $\alpha_0=-eA_0/\mu c\omega$ is the classical radius of vibration of the electron in the laser field. Let us further define the Green's function $G^0_{nn'}(x,x')$ as the solution of the inhomogenous equation

$$(E-H_n^0)G^0_{nn'}(x,x')=\delta_{nn'}\delta(x-x'), \quad (8)$$

where

$$H_n^0=-\frac{1}{2\mu}\frac{\partial^2}{\partial x^2}+\frac{1}{2}i\omega\alpha_0(S_n^+-S_n^-)\frac{\partial}{\partial x}-n\omega. \quad (9)$$

It has been shown [23] that this Green's function takes the explicit form (with the infinitesimally small and positive ϵ)

$$G^0_{nn'}(x,x')=\frac{1}{2\pi}\int_{-\infty}^{\infty}dp e^{ip(x-x')}$$
$$\times\sum_{N\in\mathcal{Z}}\frac{J_{N-n}(\alpha_0 p)J_{N-n'}(\alpha_0 p)}{E+N\omega-p^2/2\mu+i\epsilon}. \quad (10)$$

In terms of this Green's function, the solution of Eq. (5) can be expressed as

$$\psi_n(x)=\sum_{n'\in\mathcal{Z}}\int_{-\infty}^{\infty}dx' G^0_{nn'}(x,x')$$
$$\times\frac{P}{2a}\sum_{m\in\mathcal{Z}}\delta(x'-ma)\psi_{n'}(x'). \quad (11)$$

Since the crystal is periodic in space, we may invoke Bloch's theorem [17] to write $\psi_n(x)$ in the form

$$\psi_{nk}(x)=e^{ikx}\phi_{nk}(x), \quad (12)$$

where k is the quasimomentum, and $\phi_{nk}(x)$ satisfies the periodicity condition

$$\phi_{nk}(x+ma)=\phi_{nk}(x), \quad m=0,\pm1,\pm2,\ldots. \quad (13)$$

Substituting Eqs. (12) and (10) into Eq. (11), we obtain

$$\phi_{nk}(x)=-i\frac{P}{2a}\sum_{N,n'\in\mathcal{Z}}\frac{1}{p_N}J_{N-n}(\alpha_0 p_N)J_{N-n'}(\alpha_0 p_N)$$
$$\times\phi_{n'k}(0)\sum_{m\in\mathcal{Z}}e^{ip_N|x-ma|-ik(x-ma)}, \quad (14)$$

where

$$p_N=\sqrt{2\mu(E+N\omega)}, \quad (15)$$

and we have used the fact that

$$\phi_{n'k}(ma)=\phi_{n'k}(0). \quad (16)$$

We note that for sufficiently large negative values of N, corresponding to virtual emission processes, p_N could be purely imaginary. This situation is well known in the scattering theory, and corresponds to the closed-channel boundary condition with positive imaginary p_N (e.g., [24,25]). Setting $x=0$ in Eq. (14), and carrying out the sum over m, we finally arrive at [21,22]

$$\sum_{N\in\mathcal{Z}}\left[\delta_{NN'}-\frac{P}{2p_N a}J_{N-N'}(\alpha_0(p_N-p_{N'}))\right.$$
$$\left.\times\frac{\sin p_N a}{\cos ka-\cos p_N a}\right]a_N(E(k))=0, \quad (17)$$

in which the constants a_N are expressed in terms of $\phi_{nk}(0)$,

$$a_N(E(k))=\sum_{n\in\mathcal{Z}}J_{N-n}(\alpha_0 p_N)\phi_{nk}(0), \quad (18)$$

where we have explicitly marked the functional dependence of the quasienergy E on the quasimomentum k.

In the absence of the laser field the system of algebraic equations (17) decouples into

$$\left[1-\frac{P}{2p_N a}\frac{\sin p_N a}{\cos ka-\cos p_N a}\right]a_N(E(k))=0, \quad N\in\mathcal{Z}. \quad (19)$$

If we now assume that in the field-free case ($F_0=0$) the electron's energy is $E(k)$, then $N=0$ and Eq. (19) yields the classic dispersion relation [19] of the field-free Kronig-Penney model

$$\cos ka=\cos p_0 a+\frac{P}{2p_0 a}\sin p_0 a, \quad (20)$$

with $p_0=\sqrt{2\mu E(k)}$ and

$$a_N(E(k))=\mathcal{N}\delta_{N0}, \quad (21)$$

where $\mathcal{N}$ is a normalization constant of the Bloch state.

For a nonvanishing laser field, Eq. (17) shows that the quasienergy $E(k)$ fulfills the exact dispersion relation

$$\det\left[\delta_{NN'}-\frac{P}{2p_N a}J_{N-N'}(\alpha_0(p_N-p_{N'}))\frac{\sin p_N a}{\cos ka-\cos p_N a}\right]=0. \quad (22)$$

Notice that the roots of Eq. (22), or the quasienergies $E(k)$ as a function of k, appear in p_N [c.f. Eq. (15)]. This result permitted [21,22] us to derive two general theorems regarding the laser-modified energy bands, which are valid for any frequency or intensity of the laser field: (a) the Floquet-band theorem, which states that if $E(k)$ is a solution of the dispersion relation (22) then $E(k)+M\omega$ with an arbitrary integer M, is also a solution; and (b) the Kramer's theorem, which

says that if $E(k)$ is a solution of Eq. (22) then $E(-k)$ is also a solution of this equation, and $E(k)=E(-k)$, i.e., the band structure is symmetric about $k=0$.

These two general theorems have important practical implications. Theorem (a) implies that a given exact Floquet band must be parallel to all the M replicas associated with it. From the computational point of view the infinite matrix in Eq. (22) has to be truncated in Floquet-Fourier space n. Such a truncation in general violates the Floquet-band theorem in the sense that it is only approximately fulfilled up to some finite range of M. If the initial truncation is too drastic, then one has to increase the number of Floquet-Fourier channels to ensure a given degree of parallelism of the calculated quasienergy bands. The Kramer's theorem (b) implies that only odd harmonics are radiated in the thin-film case. These points are discussed below in greater details in connection with concrete calculations.

III. BAND STRUCTURES OF A CLASS OF KRONIG-PENNEY-TYPE MODELS

In Sec. II we analyzed an exactly soluble model of the interaction of electrons with both a space periodic crystal potential and a time periodic laser field. In this section we introduce a more general class of periodic potentials using finite quare wells, and discuss the modification of the band structure of the system in the presence of a strong laser field. We define

$$V(x)=\begin{cases} V_1, & \frac{1}{2}b+m(a+b)<x<\frac{1}{2}b+a+m(a+b) \\ V_2, & -\frac{1}{2}b+m(a+b)<x<\frac{1}{2}b+m(a+b), \end{cases} \tag{23}$$

with an integer m. This model reduces to the Kronig-Penney model in the limit $(b,V_1)\rightarrow 0$ and $V_2\rightarrow\infty$, with $V_2 b=P/2a$ kept constant. Although this model is not analytically exactly soluble as the previous one, it also permits us to analyze efficiently the band structure in a strong laser field, as was first shown in [26]. In addition, it contains more parameters than in the Kronig-Penney model of Sec. II, that allow one more conveniently to model a given system of interest.

A. Floquet-Bloch band, mean band-spectrum, band dispersion, and band entropy

The mathematical formulation of the Floquet-Bloch calculations of the band structure in the presence of an intense laser field is discussed in details in the Appendix, where it is shown how this problem can be reduced to an eigenvalue problem [26], Eq. (A14), of the type

$$\mathcal{F}C=e^{ikl}C, \tag{24}$$

where, $\mathcal{F}$ is the so-called Floquet-Bloch matrix [26] that depends on the quasienergy E; k is the quasimomentum; and C are the eigenvectors associated with the Floquet-Bloch states $\psi_{\beta k}(x,t)$, with $\beta=1,2,3,\ldots$ labeling the bands. For the purpose of concrete numerical simulations we have taken the model parameters as follows: $a=2.2715$, $b=6.8145$ a. u., $V_1=-15.203$ eV, and $V_2=-7.451$ eV.

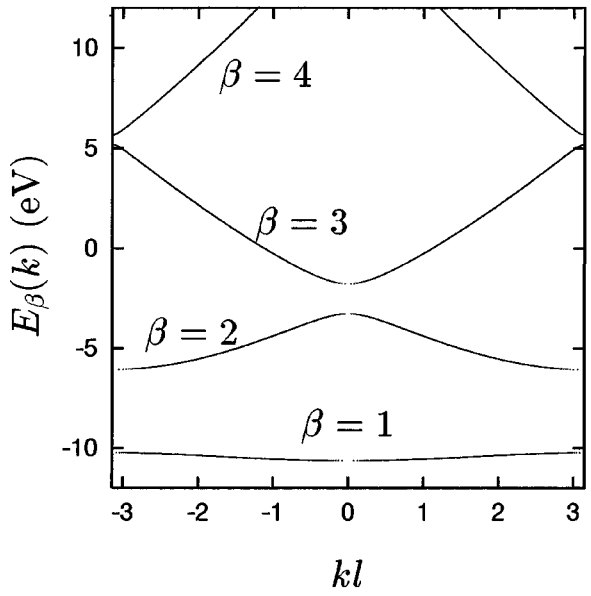

FIG. 2. The field-free band structure for the one-dimensional crystal potential, Eq. (23). The dots appearing in the band structure in this figure (and in the subsequent figures) are due to limited density of points in the computations; they may be connected smoothly by interpolation, if desired.

In Fig. 2 we present the calculated unperturbed band structure and, the minimum and maximum energy values for the bands are given in Table I. It can be seen, for example, that with the above choice of parameters, for a one-and-half-filled crystal (i.e., fully filled first band and half-filled second band), one obtains a Fermi energy $E_F=5.53$ eV that is comparable to that of gold [29]; a crystal that has been used, e.g., in the experiment of Farkas *et al.* [4].

In the presence of the time-periodic laser field the band structure has a multivalued representation corresponding to the different Floquet zones within a given (e.g., the first) Brillouin-zone. The simultaneous occurence of the Brillouin- and Floquet zones is a general feature of the band-structure calculations in the presence of the field, and, as discussed in Sec. II is a consequence of the simultaneous presence of the spatial and time-periodic interactions in the system. In order to anticipate in which way the band structure would be modified in the presence of the field, it is useful first to consider the unperturbed band structure in the Floquet (or the so-called ''dressed'') picture, as shown in Fig. 3, which is

TABLE I. The minimum and maximum energies $E_{\min}$ and $E_{\max}$, respectively, for the field-free band (index β) calculated for the periodic potential defined by Eq. (23). Note that in this case the middle of the second band occurs at an energy -5.1 eV, which for a one-and-half-filled crystal corresponds to a Fermi energy $E_F=5.53$ eV, similar to that for gold [29].

β	$E_{\min}$ (eV)	$E_{\max}$ (eV)
1	−10.630	−10.230
2	−6.062	−3.273
3	−1.776	5.187
4	5.677	16.547
5	16.907	30.947

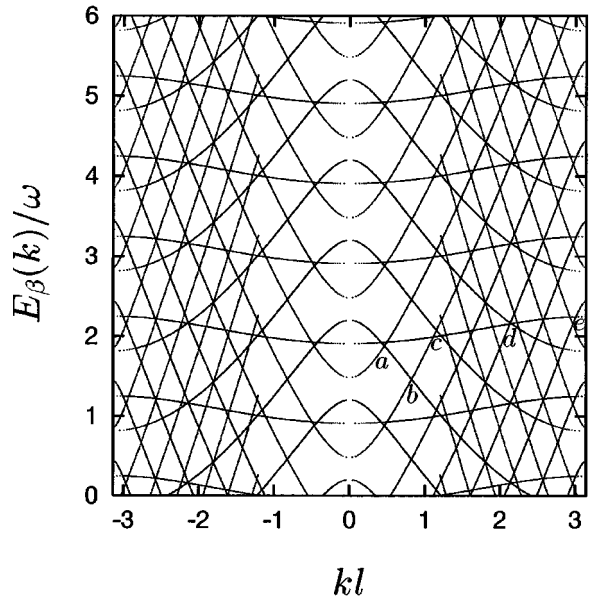

FIG. 3. Floquet replication of the field-free band structure given in Fig. 2. The first six Floquet zones at the interval of the photon energy $\omega=1.169$ eV are shown. The crossings of the bands marked by small letters correspond to the resonant transitions: (a) and (b) for the two- and three-photon resonant transitions between the second and third bands, (c) and (d) for the five- and four-photon resonant transitions between the first and second bands, and (e) for the one-photon resonant transition between the third and fourth bands.

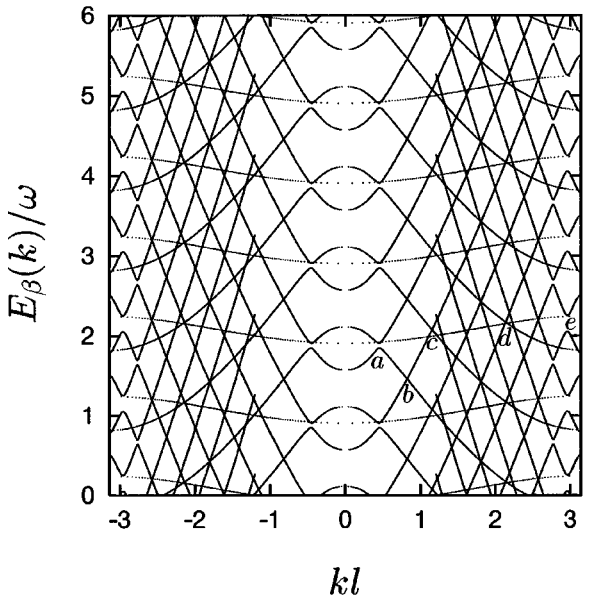

FIG. 4. The Floquet-Bloch band structure in the presence of the field at an intensity $I=3.51\times10^{10}$ W/cm^2 and a photon energy $\omega=1.169$ eV. Note that the field-free crossings (e) and (a) in Fig. 3 become the avoided crossings now in the presence of the field. We note also that an avoided crossing is broader for a resonance due to a smaller number of photons exchanged. The crossings (b), (c), and (d) are in fact narrow anticrossings. Observe that the calculated spectrum passes continuously from one Floquet zone to another, implying a good convergence of the calculations with respect to the truncation in the Floquet (or photon) space.

readily obtained by replicating the unperturbed spectrum at an interval of the photon energy. Note in particular that in this representation the bands are characterized by crossing points, some of which are indicated (a)–(e) in the figure. They represent the unperturbed positions of possible interband resonances that may occur due to the absorption and emission of photons in the presence of the field.

This unperturbed Floquet band structure is to be compared with the Figs. 4 and 5, where we show the calculated band structure in the presence of the field, for two selected intensities, $I=10^{-6}$ and 10^{-5} a.u. respectively. (Note that 1 a.u. of intensity corresponds to 3.51×10^{16} W/cm^2). At the relatively lower intensity of $I=10^{-6}$ a.u. the resonance (a) shows up as an anticrossing (Fig. 4), where the other resonances are not resolved. At $I=10^{-5}$ a.u., which is one order of magnitude larger, we observe that all the resonances (a)–(e) appear strongly with well-resolved anticrossings (Fig. 5).

As an alternative to the description of the multivalued Floquet-Bloch band structure, we introduce the useful concept of a ''mean-band spectrum.'' We define this quantity as the quantum expectation value of the energy operator with respect to the Floquet-Bloch states. Thus let the expectation value with respect to a given Floquet-Bloch state $\psi_{\beta k}(x,t)$ be

$$\mathcal{E}_\beta(k)=\frac{1}{T}\int_0^T dt\int_0^l dx\,\psi^*_{\beta k}(x,t)i\partial_t\psi_{\beta k}(x,t), \tag{25}$$

where $T=2\pi/\omega$, and ω is the frequency of the laser field. If the Floquet-Bloch state is normalized as

$$\frac{1}{T}\int_0^T dt\int_0^l dx|\psi_{\beta k}(x,t)|^2=1, \tag{26}$$

then the *mean energy* $\mathcal{E}_\beta(k)$ can be expressed as

$$\mathcal{E}_\beta(k)=\sum_{N\in\mathcal{Z}}[E_\beta(k)+N\omega]P_{\beta N}(k), \tag{27}$$

where the real number $P_{\beta N}(k)$, which satisfies

$$\sum_{N\in\mathcal{Z}}P_{\beta N}(k)=1, \tag{28}$$

can be interpreted as the probability that the electron in the laser field, being in the Floquet-Bloch state $\psi_{\beta k}(x,t)$, has the energy $E_\beta(k)+N\omega$. In the above equations we have explicitly marked the dependence of the quasienergy $E_\beta(k)$ on the Bloch quasimomentum k, and indicated a band index β.

The mean band energy $\mathcal{E}_\beta(k)$ defined above is a single-valued ''structure quantity'' in the following sense. The Floquet theorem discussed in Sec. II states that independently of whether we define the Floquet-Bloch matrix $\mathcal{F}$ in Eq. (24) for the quasienergy E or $E+M\omega$ with an integer M, we always obtain the same set of eigenvalues of Eq. (24), or the same set of quasimomenta. Due to this theorem, the quasienergy can be always reduced to the first Floquet zone $[0,\omega)$; had we chosen, for instance, the interval $[\omega,2\omega)$, we would have gotten exactly the same results. This is why the quasienergy itself does not have an invariant meaning for the crystal, or, in other words, is not a ''structure quantity.'' In contrast, independently of the choice of the quasienergy, whether it is E or $E+M\omega$, the same value is obtained for the mean energy, and hence it represents an invariant structure

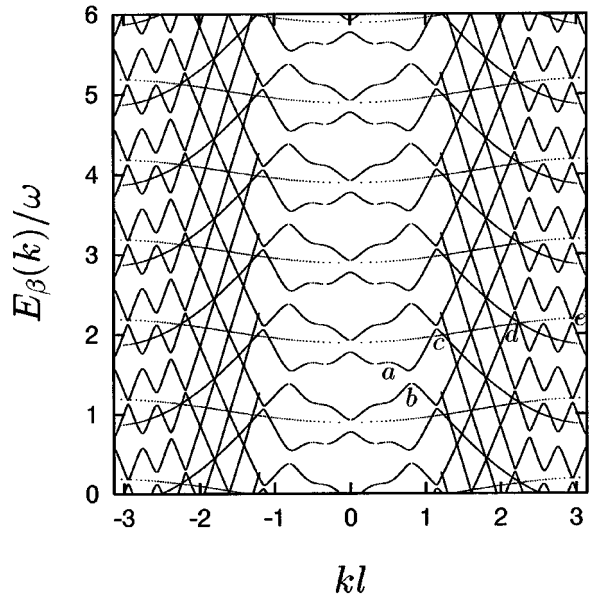

FIG. 5. The same as in Fig. 4, but for a much larger intensity $I=3.51\times10^{11}$ W/cm^2. Observe that the three-photon avoided crossing (b) now becomes broader and visible, whereas the one-photon avoided crossing (e) becomes narrower than at the smaller intensity. On the other hand, the two-photon avoided crossing (a) of Fig. 4 now shows a nonmonotonic dependence of the quasienergy on the quasimomentum. These characteristics indicate strong nonperturbative response of the crystal even at this not very large intensity.

quantity of the crystal in the presence of the field. Mathematically the invariance of the mean energy spectrum is ensured due to the fact that the transformation

$$E\rightarrow E+M\omega \tag{29}$$

implies the transformation

$$P_{\beta N}(k)\rightarrow P_{\beta,N+M}(k), \tag{30}$$

[see Eq. (A29) and rules (A17) and (A18)]. [In the particular case of the vanishing laser field, the mean energy $\mathcal{E}_\beta(k)$ goes over exactly to the unperturbed eigenvalues.] In Fig. 6 we show the mean energy spectrum at two nonvanishing values of the field intensity, $I=3.51\times10^{10}$ and 3.51×10^{11} W/cm^2, and compare them with that in the absence of the field ($I=0$). One of the more interesting features seen in these figures is the formation of minigaps at the points where the bands are resonantly coupled by the laser field. For the small laser intensity, the widths of the minigaps [21,22,26] are seen to increase with the intensity. This can be understood from a consideration of the well-known two-level dynamics. Thus a resonantlike situation may be approximated by a two-state Hamiltonian. If a pair of states are resonantly coupled, then one observes the so-called Autler-Townes splitting of the quasienegy associated with the Rabi oscillations of the occupation probability between the coupled states, which for small intensities is proportional to the intensity of the laser field. For larger intensities instead of the linear growth, we observe a modulation of the splitting as a function of the intensity, which can include a number of ''zero splittings'' for some particular values of intensities [8]. Exactly this type of behavior is observed for the minigaps (a) and (e). Further, for sufficiently high intensity some bands (in our case the second band) exhibit a new phenomenon (which cannot occur in one-dimensional periodic structures in the absence of the laser field). That is, in some regions of the k space, e.g., near the (a), the bands become multivalued, or show a nonmonotonic behavior, implying more than one positive quasimomenta having the same quasienergy.

Besides the mean energy, the band structure in the presence of the field can be further characterized by the second (or higher) moments of the energy distribution in the Floquet space. Thus we define, the *standard deviation* of the distribution,

$$\sigma_\beta(k)=\sqrt{\sum_{N\in\mathcal{Z}}[E_\beta(k)+N\omega]^2P_{\beta N}(k)-[\mathcal{E}_\beta(k)]^2}. \tag{31}$$

Alternatively, we can define a *band entropy* as

$$S_\beta(k)=-\sum_{N\in\mathcal{Z}}P_{\beta N}(k)\ln P_{\beta N}(k). \tag{32}$$

Each of these quantities provide a measure of the dispersion of the *band energy* in photon space. The standard deviation at two diffrent laser intensities are presented in Figs. 7 and 8, and those for the band entropy are shown in Figs. 9 and 10, repectively. We see that any resonance (avoided crossing)

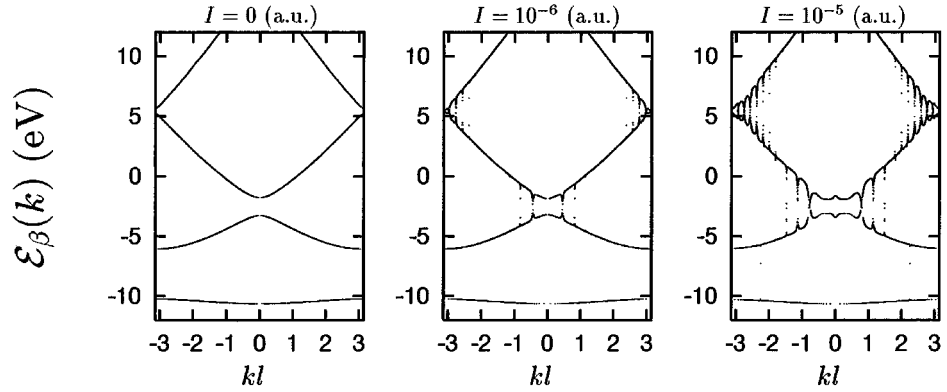

FIG. 6. The single-valued spectrum of the mean band energy $\mathcal{E}_\beta(k)$ (in eV). Compare the field-free case ($I=0$), with that in the presence of the field: 3.51×10^{10} and 3.51×10^{11} W/cm^2 at $\omega=1.169$ eV.

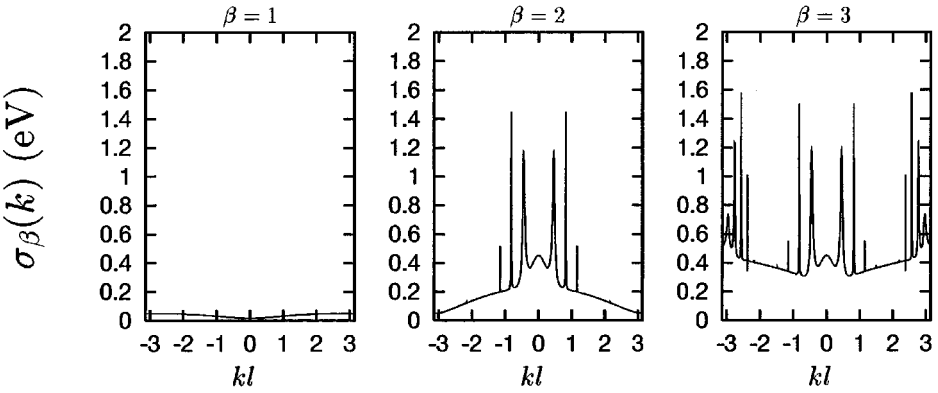

FIG. 7. The standard deviations $\sigma_\beta(k)$ of the fluctuation of the band energy in the Floquet space (see text for the definition) in eV for the three lowest bands as a function of the dimensionless quasimomentum kl and an intensity $I=3.51\times10^{10}$ W/cm^2. Observe, the sharp increase at the resonances, indicating that the probabilities $P_{\beta N}(k)$ at these values of k and β disperse strongly in N.

between the bands shows up unmistakenly, both in the standard deviation and in the band entropy as a sharp peak. This allows us to identify the resonances, even when they are sharp, very conveniently. It also shows that at these quasimomenta the probabilities $P_{\beta N}(k)$ are strongly dispersed in N, implying significant absorption or emission of large number of photons. Note that now even the very narrow avoided crossings [e.g., the crossing of the second and the third bands next to (b) in Fig. 4, or the crossing (d), between the first and the second bands, in Fig. 5] can be easily identified. Note also that in the Fig. 5 the disappearance of the avoided crossing (a) leads to the disappearance of the corresponding peak in the standard deviation (Fig. 8), showing a one-to-one correspondence between the two quantities.

IV. HIGH-HARMONIC SPECTRUM

The fundamental physical process for the emission of high-harmonic radiation is the forced oscillation of the induced band current due to the laser field, which can depart from a pure sinusoidal oscillation due to nonlinear interaction with the lattice potential. The Floquet-Bloch wave function and the associated currents derived below according to the present theory, can now be used to investigate the high-harmonic generation process in a crystal in a fully nonperturbative way.

A. Floquet-Bloch current; definition of high-harmonic spectrum

We define the high-harmonic power spectrum quantitatively by the Fourier transform of the expectation value of the probability current density integrated over the elementary cell. It can be written as (cf. [27])

$$\frac{dS}{d\Omega}=\frac{\alpha^3}{3\pi}\left|\sum_\beta\sum_{|k|\le k_F}\int_{-T_0/2}^{T_0/2}dt e^{i\Omega t}\times\frac{d}{dt}\left[N_c\int_0^l dx\, j_{\beta k}(x,t)\right]\right|^2, \tag{33}$$

in which $N_c l=L$ is the effective length of the crystal, $\alpha\approx\frac{1}{137}$ is the fine-structure constant, T_0 is the time duration of the laser pulse, and

$$j_{\beta k}(x,t)=\frac{1}{2\mu}\left(\psi^*_{\beta k}(x,t)\left[\frac{1}{\mathrm{i}}\partial_x-\frac{e}{c}A(t)\right]\psi_{\beta k}(x,t)+\psi_{\beta k}(x,t)\left[-\frac{1}{\mathrm{i}}\partial_x-\frac{e}{c}A(t)\right]\psi^*_{\beta k}(x,t)\right) \tag{34}$$

is the Floquet-Bloch current density. The summations extends over quasimomenta of the occupied bands, and over

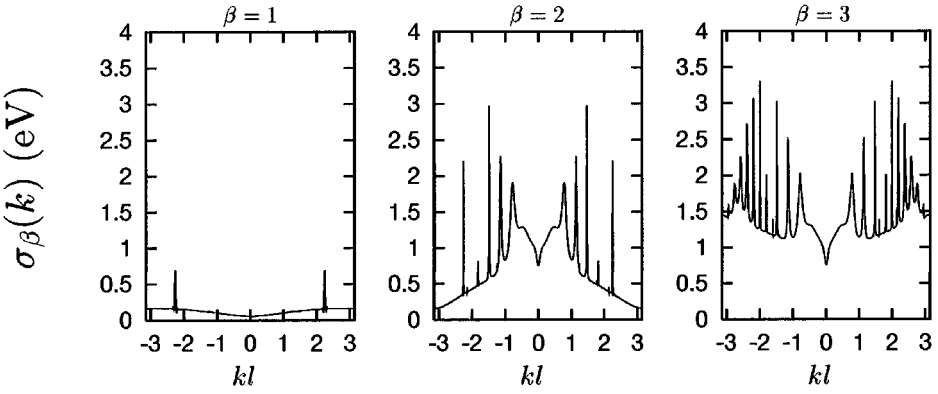

FIG. 8. The same as in Fig. 7, but for a larger intensity $I=3.51\times10^{11}$ W/cm^2. For this intensity one clearly sees a four-photon resonant transition between the first and second bands for $kl\approx\pm2.2$. Note also a weak five-photon resonance which is barely visible at $kl\approx\pm1.2$.

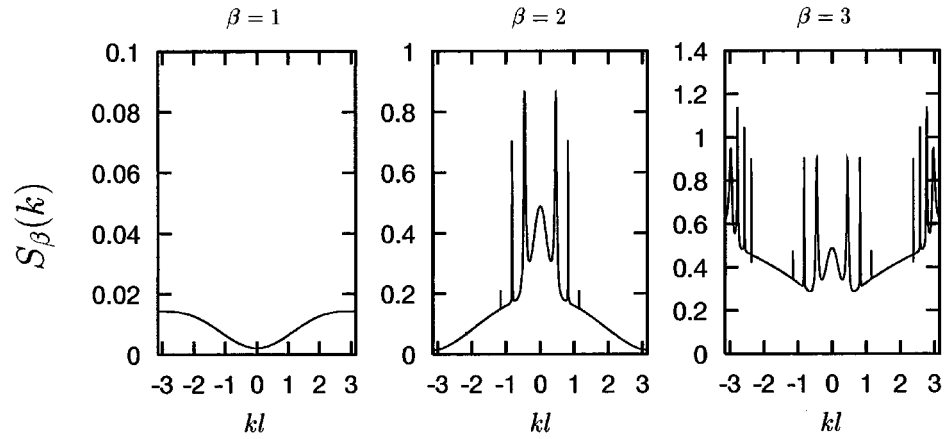

FIG. 9. The same as in Fig. 7, except that the quantity plotted is the band entropy (see the text for the definition).

such quasimomenta of the partially occupied band that are equal to or smaller than the Fermi momentum k_F.

We Fourier analyze the Floquet-Bloch probability current density integrated over an elementary cell, Eq. (34), to obtain

$$\int_0^l dx\, j_{\beta k}(x,t)=\sum_{N\in\mathcal{Z}} e^{-iN(\omega t+\delta)}\mathcal{J}_{\beta N}(k), \tag{35}$$

where

$$\mathcal{J}_{\beta N}(k)=\Bigg[\mathcal{N}_{\beta k}^{-1}\sum_{i=1}^{i_0}\sum_{\sigma,\sigma'=\pm}\sum_{n,n'\in\mathcal{Z}}\frac{\sigma p_{\beta in}+\sigma' p^*_{\beta in'}}{2\mu} \times J_{n'-n+N}(\sigma\alpha_0 p_{\beta in}-\sigma'\alpha_0 p^*_{\beta in'}) \times n_i(\sigma p_{\beta in}-\sigma' p^*_{\beta in'})C_{in}^{\beta\sigma}(C_{in'}^{\beta\sigma'})^*\Bigg] + \tfrac{1}{2}\omega\alpha_0[\rho_{\beta,N-1}(k)+\rho_{\beta,N+1}(k)], \tag{36}$$

and $\rho_{\beta N}(k)$ are defined in the appendix, Eq. (A26). In the limit of large T_0 (compared to the period of the field) the rate of emission of high-harmonic radiation $dW/d\Omega$, Eq. (33), at the frequency Ω takes the form

$$\frac{dW}{d\Omega}=\frac{1}{T_0}\frac{dS}{d\Omega}=\frac{2}{3}\alpha^3 N_c^2\sum_{N\in\mathcal{Z}}\delta(\Omega-N\omega)S_N(k_F), \tag{37}$$

where

$$S_N(k_F)=\Bigg|\sum_\beta\sum_{|q|\le q_F} D_{\beta N}(q)\Bigg|^2, \tag{38}$$

$$D_{\beta N}(q)=N\omega\mathcal{J}_{\beta N}(k), \tag{39}$$

is the Nth Fourier component of the current, N_c is the effective number of elementary cells in the laser focus, α is the fine-structure constant, and $q=kl$ is the dimensionless quasimomentum. It should be noted that $D_{\beta N}(q)$ are real, which follows from the explicit form of $\mathcal{J}_{\beta N}(k)$ given by Eq. (36).

The dependence of the current distribution functions, Eq. (39), on the quasimomentum is shown in Figs. 11 and 12 for two different intensities and for several odd values of N. Since

$$D_{\beta N}(-q)=(-1)^{N+1}D_{\beta N}(q), \tag{40}$$

therefore for even N these functions are antisymmetric and their integration with respect to q over the occupied Brillouin zones, cancells out in Eq. (38). Thus, no even harmonics can radiate in this case, as is to be expected from the inversion symmetry of the periodic structure considered. In Figs. 11 and 12 we see that any resonance which occurs in the band structure (see, Figs. 4 and 5) is represented here by a rapid change of the current. Such a behavior is expected to lead to

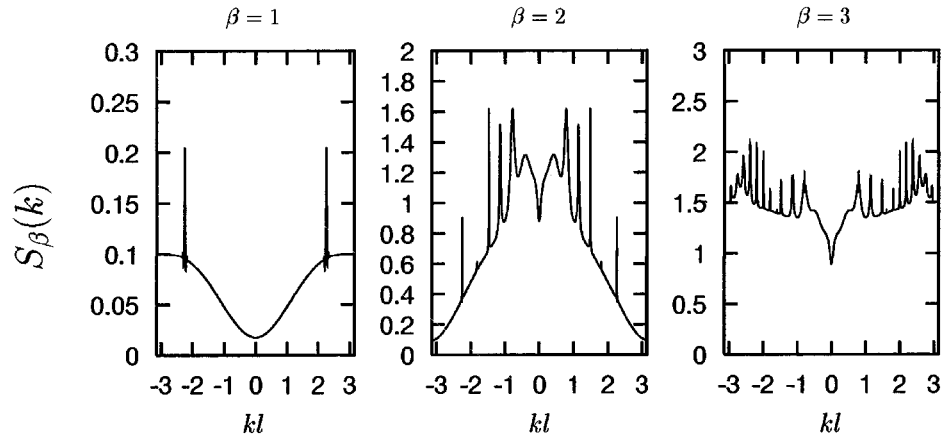

FIG. 10. The same as in Fig. 8, except that the quantity plotted is the band entropy (see the text for the definition).

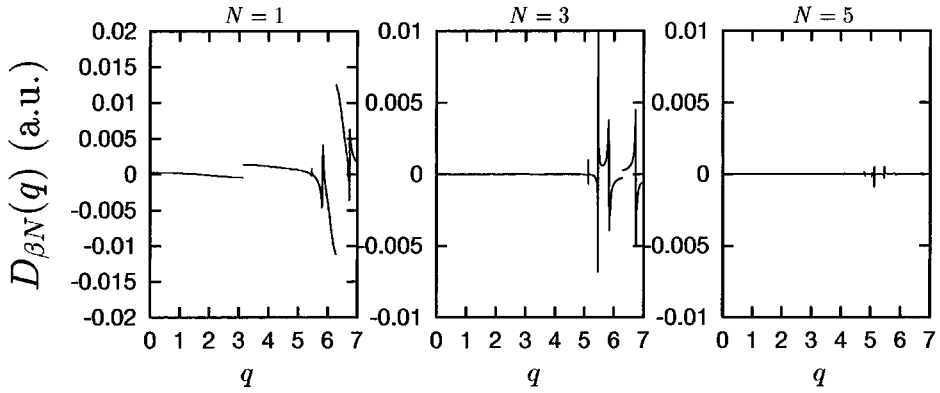

FIG. 11. The harmonic component of the current distribution [see Eq. (39) in text] $D_{\beta N}(q)$ (in a.u.) as functions of the dimensionless quasimomentum $q=kl$ for harmonic orders N at an intensity $I=3.51\times10^{10}$ W/cm^2. $D_{\beta N}(q)$ are shown in the extended zone representation. Observe the presence of the discontinuities at $q=\pi$ and 2π, which are connected with the passage from the first to the second band and from the second to the third band, respectively. Note also the rapid changes in the current distribution functions at the resonances.

a significant modification of the power spectrum of the harmonics, defined by $S_N(k_F)$, Eq. (38), when the Fermi momentum k_F is in the close vicinity of the quasimomentum corresponding to the resonant transition. Let us note, however, that due to the interference effects of different N components one may observe either enhancement or supression of the higher harmonics near the interband resonances [28].

B. High-harmonic spectra

We calculate the high-harmonic power spectrum for three types of crystals: (a) insulator, e.g., when initially only the first band is occupied and there is a wide gap between the valence and the conduction bands; (b) metal, e.g., when initially the second band is half-filled by electrons; and (c) semiconductor, e.g., when the second band is completely filled and there is a narrow gap between the valence and conduction bands. The results obtained at two different intensities are presented in Figs. 13 and 14. We see that (Fig. 13), for $I=10^{-6}$ a.u. (i.e., 3.51×10^{10} W/cm^2), the strength of the emitted power drops down approximately linearly (in the logarithmic scale) with the order N. This behavior is consistent with the expectation based on the perturbation theory, i.e., with the power law

$$S_N(k_F)\approx S_0(I/I_{\rm trn})^N, \tag{41}$$

where S_0 is a constant, and $I_{\rm trn}$ may be called a ''transition intensity'' between a perturbative and a nonperturbative domain for harmonic generation. Since

$$\ln\frac{S_N(k_F)}{S_0}\approx N\ln\frac{I}{I_{\rm trn}}, \tag{42}$$

therefore, from the slopes of lines in Fig. 13 we estimate that $\ln(I/I_{\rm trn})\approx-2$. This indicates that a transition intensity in solids, is of the order of 10^{-4} a. u. or 3.5×10^{12} W/cm^2, and that this is essentially the same irrespective of the initial field-free conduction properties. The nonperturbative effects can already be seen in Fig. 14, for $I=10^{-5}$ a.u. (3.51×10^{11} W/cm^2), where it can be seen that for semiconductors the third harmonic is in fact stronger than the elastically scattered radiation at the fundamental (first peak). It is interesting to note that a similar dominance of the third harmonic, over the elastically scattered radiation, can also be seen to occur in an earlier calculation [6] for a semiconductor. In the case of the metal and the insulator, Fig. 14 shows that the strength of the fifth harmonic is comparable with that of the third harmonic. From Figs. 13 and 14 it can be seen that, at the intensities investigated here, the semiconductor films are likely to generate relatively higher harmonics with greater efficiency than either metals or insulators.

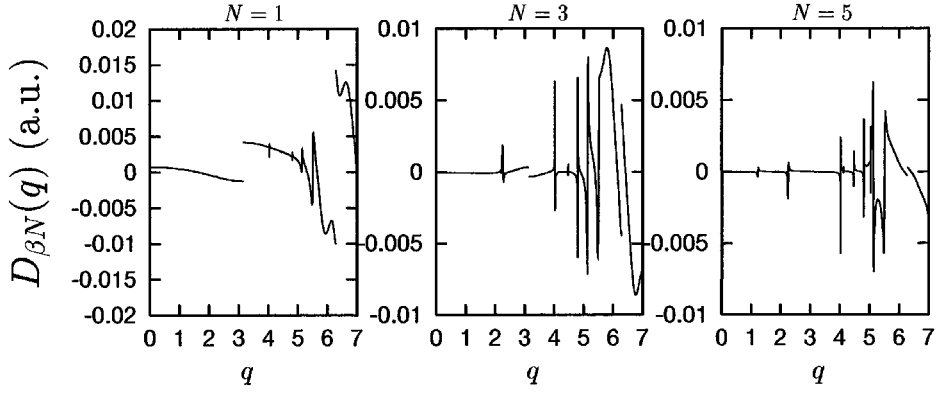

FIG. 12. The same as in Fig. 11, but for a larger intensity $I=3.51\times10^{11}$ W/cm^2. Observe a well developed five-photon resonant transition between the first and second bands at $q\approx1.2$.

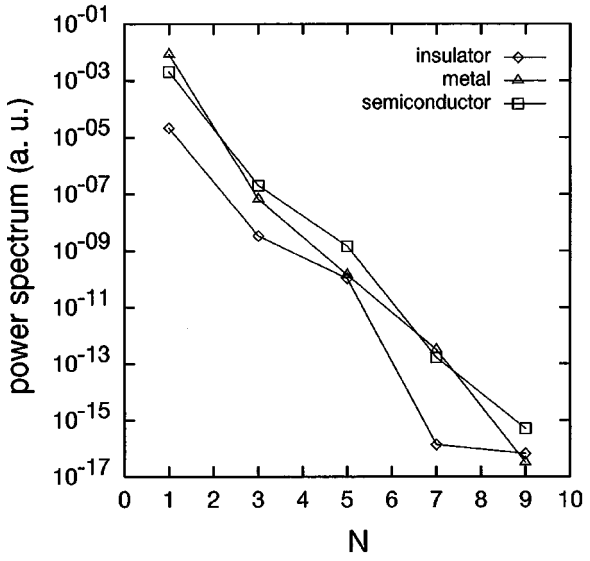

FIG. 13. The high-harmonic power spectrum $S_N(k_F)$ (in a.u.) at an intensity $I=3.51\times10^{10}$ W/cm^2 for three different Fermi momenta k_F corresponding to an insulator ($k_F l=\pi$), a metal ($k_F l=3\pi/2$), and a semiconductor ($k_F l=2\pi$). Notice the essentially perturbative character of this spectrum, showing a general rapid decrease of the signal with increasing orders of the harmonic.

V. SUMMARY AND PROSPECTS

To summarize, we have developed a Floquet-Bloch theory of nonperturbative analysis of a periodic electronic structure, such as a crystal or a thin film, interacting with an intense laser field. The theory is used to determine the modification of the band structure, the mean energy spectrum of the band, the standard deviation of the band energy in the photon space, and the associated band entropy. The last two quantities provide useful measures of the fluctuation in the distribution of the band energy in the photon (or Floquet) space as well as identifying the multiphoton interband resonances. The numerical results are used to demonstrate the occurrence of minigaps and the influence of the interband resonances on the Fourier component of the current distribution in a laser-modified (Floquet-Bloch) band. Finally, the power spectrum of high-harmonic generation is investigated for different types of crystal media, and their dependence on both perturbative and nonperturbative intensities is studied. It is shown that thin films or crystals, irrespective of their conduction properties (i.e., insulators, metals or semiconductors), are very efficient in generating higher harmonics at moderate intensities. A transition intensity for strong harmonic generation in such crystals is found to be the order of 3.51×10^{12} W/cm^2. It is also found that for Nd:YAG lasers both at $I=3.51\times10^{10}$ and 3.51×10^{11} W/cm^2, a semiconductor medium is comparatively more efficient in generating higher harmonics than either an insulator or a metal film. Finally, we note that the theory developed here permits one to analyze a whole class of related problems of interaction of intense lasers with periodic structures, and that this has been recently fruitfully applied to the problem of laser interaction with transmission electrons in a crystal [10] which led to the prediction of a phenomenon of multiple plateaus in high-harmonic spectra, due to induced interband resonances.

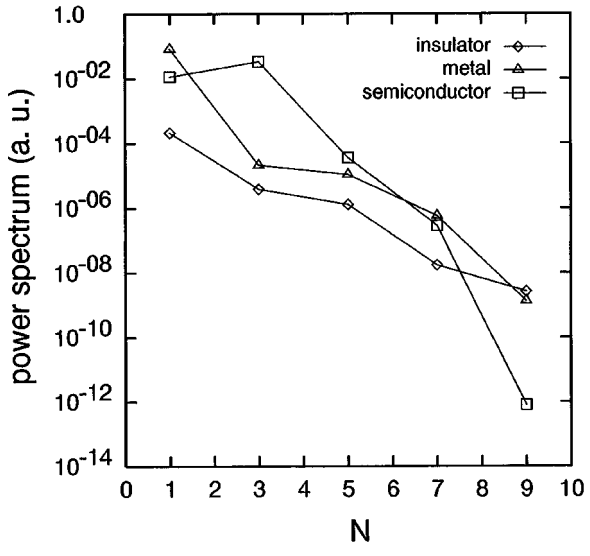

FIG. 14. The same as in Fig. 13, but for a larger intensity $I=3.51\times10^{11}$ W/cm^2. Observe that at this intensity the harmonic spectrum behaves rather nonperturbatively.

ACKNOWLEDGMENTS

This work was supported partially by the Deutche Forschungsgemeinshaft, Bonn. One of the authors (J.Z.K.) was supported in part by the Polish Committee for Scientific Research under Grant No. KBN 2 P302 070 07.

APPENDIX: BAND STRUCTURE AND FLOQUET-BLOCH STATES

The aim of this appendix is to present the method used to determine the Floquet-Bloch states and the band structure for an arbitrary one-dimensional potential, that is constant in finite intervals. Such a potential can be described by two sets of real numbers: $\{x_i\}_{i=0,1,\ldots,K}$ and $\{V_i\}_{i=1,\ldots,K}$, in which V_i is the value of the potential in the interval $[x_{i-1},x_i]$. It is well known how to treat the field-free problem for such potentials. One divides the space into K nonoverlapping domains, and for each of these domains writes down the most general form of the wave function, which is a linear combination of two counterpropagating plane waves. The complex coefficients that multiply these plane waves are then determined up to a normalization constant from the matching conditions (i.e., from the continuity of the wave function and of its space derivative), whereas the band structure follows from Bloch's periodicity condition. It appears that a similar method can be applied to an analysis of the band structure in the presence of a monochromatic electromagnetic plane waves. However, in order to do this we have to know the most general solution of the time-dependent Schrödinger equation (the units in which $\hbar=1$ are used here),

$$i\partial_t\Psi=\left[-\frac{1}{2\mu}\frac{\partial^2}{\partial x^2}+\frac{ie}{\mu c}A(t)\frac{\partial}{\partial x}+\frac{e^2}{2\mu c^2}A^2(t)+V(x)\right]\Psi, \tag{A1}$$

or, after the unitary transformation, Eq. (3), of the equation,

$$i\partial_t\psi=\left[-\frac{1}{2\mu}\frac{\partial^2}{\partial x^2}+\frac{ie}{\mu c}A(t)\frac{\partial}{\partial x}+V(x)\right]\psi, \tag{A2}$$

in the different domains of constant $V(x)$. In this equation the time-dependent vector potential $A(t)$ describes a plane wave in the dipole approximation

$$A(t)=A_0\cos(\omega t+\delta), \tag{A3}$$

with an arbitrary phase δ, and $V(x)$ is a static periodic potential which is chosen to model the crystal lattice [30]. Note, that the $A^2(t)$ term, which can be eliminated by the space-independent unitary transformation, does not change the band structure and can be taken into account in the wave function, if desired, by the back transformation (3). A general solution of Schrödinger equation (A2), with $V(x)$ defined above, that accounts for the periodicity of the Hamiltonian in time, is of the form [31] (cf., [32,33])

$$\psi^{(i)}(x,t)=e^{-iEt}\sum_{n,N\in\mathcal{Z}} e^{-iN(\omega t+\delta)}[J_{N-n}(\alpha_0 p_{in})e^{ip_{in}x}C_{in}^{+} + J_{N-n}(-\alpha_0 p_{in})e^{-ip_{in}x}C_{in}^{-}], \quad x_{i-1}<x<x_i, \tag{A4}$$

in which $\mathcal{Z}=0,\pm1,\pm2,\ldots$, $J_n(z)$ are the Bessel functions, $\alpha_0=-eA_0/\mu c\omega$, and C_{in}^{+} and C_{in}^{-} are arbitrary complex constants, E is the so-called quasienergy (Floquet characteristic exponent), and

$$p_{in}=\sqrt{2\mu(E-V_i+n\omega)}. \tag{A5}$$

It is clear that, for the field-free problem, when $\alpha_0=0$ and $N=0$, this solution reduces to the superposition of two counterpropagating plane waves of energy E. However, for a nonvanishing laser field the structure of this solution becomes much more complicated, because instead of two arbitrary constants it now contains an infinite number of them, which makes computations much more difficult. Moreover, this solution contains the so-called closed channels, for which the momenta p_{in} defined by Eq. (A5) become complex. It is well known from scattering theory, e.g., [24], that such closed channels—although not directly accessible to free motion of the electron—play a very important role both in principle—for instance, one cannot satisfy the probability conservation law without taking them into account—and in physical effects, e.g. for the cupture-escape resonances [25] in radiative electron-ion scattering.

The matching conditions for $x=x_{i-1}$ can be written down in the matrix form

$$B(i-1,x_{i-1})C_{i-1}=B(i,x_{i-1})C_i, \tag{A6}$$

in which $C_i^{\pm}=C_{in}^{\pm}$,

$$B(i,x)=\begin{pmatrix} B^{+}(i,x) & B^{-}(i,x) \\ B'^{+}(i,x) & B'^{-}(i,x)\end{pmatrix}, \quad C_i=\begin{pmatrix} C_i^{+} \\ C_i^{-}\end{pmatrix}, \tag{A7}$$

and the matrices B and B' are defined as

$$[B^{\pm}(i,x)]_{N,n}=J_{N-n}(\pm\alpha_0 p_{in})e^{\pm ip_{in}x}, \tag{A8}$$

$$[B'^{\pm}(i,x)]_{N,n}=\pm ip_{in}J_{N-n}(\pm\alpha_0 p_{in})e^{\pm ip_{in}x}. \tag{A9}$$

Hence, we arrive at the following chain of equations for the columns C_i:

$$C_i=B_iC_{i-1}, \tag{A10}$$

where

$$B_i=[B(i,x_{i-1})]^{-1}B(i-1,x_{i-1}). \tag{A11}$$

This chain of equations connects the solution in the domain $x_{i-1}<x<x_i$ to the solution in the domain $x_{j-1}<x<x_j$ [31],

$$C_j=B_jB_{j-1},\ldots,B_{i+1}C_i=\mathcal{T}_{ji}C_i, \tag{A12}$$

where the matrix $\mathcal{T}_{ji}$ is the so-called *transfer* matrix.

We have assumed that $V(x)$ is a periodic function of x with the period equal to l. This means that there exists an index i_0 such that $V_i=V_{i+i_0}=V_{i+2i_0}=\cdots$, and $x_{i+i_0}=x_i+l$. Hence a solution of Eq. (A2) at a given time t can be built up of the Bloch wave functions of the form

$$\psi_k(x,t)=e^{ikx}u_k(x,t), \tag{A13}$$

where k is the quasimomentum and $u_k(x+l,t)=u_k(x,t)$; the quasimomentum k is defined as modulo $2\pi/l$. In our further considerations we assume that $k\in[-\pi/l,\pi/l]$. The use of Eq. (A13) in Eq. (A4) leads to the eigenvalue equation [26]

$$\mathcal{F}_{i,i_0}C_i=e^{ikl}C_i, \tag{A14}$$

in which the *Bloch-Floquet* matrix $\mathcal{F}_{i,i_0}$ is defined as

$$\mathcal{F}_{i,i_0}=\mathcal{P}_i\mathcal{T}_{i+i_0,i}, \tag{A15}$$

where

$$\mathcal{P}_i=\begin{pmatrix}\mathcal{P}_i^{+} & 0 \\ 0 & \mathcal{P}_i^{-}\end{pmatrix}, \tag{A16}$$

and $(\mathcal{P}_i^{\pm})_{Nn}=\delta_{Nn}\exp(\pm ip_{in}l)$. This is the eigenvalue equation which determines the dispersion relation $E=E(k)$, and the columns C_i which are necessary for the construction of the explicit form of the Floquet-Bloch wave functions.

The eigenvalue equation (A14) consists of an infinite system of linear algebraic equations. In practical calculations such a system has to be truncated. This means that the indices N and n in Eq. (A4) run over a finite subset of integers $\mathcal{Z}$. Of course, such a truncation also reduces the number of eigenvalues and modifies their numerical values. Therefore, we require a criterion of choosing only those eigenvalues which are insensitive to the truncation. One possibility is to carry out the calculation for two subsets of integers $\mathcal{Z}_0$ and $\mathcal{Z}_1$, such that $\mathcal{Z}_0\subset\mathcal{Z}_1$, and choose, for a given quasienergy E, those quasimomenta k that lie within a prescribed error margin. This criterion was applied in [26]; its advantage consists in the rapid numerical calculation of the laser-modified band structure. However, for the purpose of this paper, we need, apart from accurate eigenvalues, also accurate values of the Floquet-Bloch wave functions. To reach this end we choose an alternative criterion based on the accuracy of the extreme components of the eigenvectors. Thus we first calculate the eigenvectors C_i of Eq. (A14), by truncating the

infinite columns $C_i^{\pm}(n)$, $n=-\infty,\ldots,+\infty$ to finite ones with $n=n_{\min},\ldots,n_{\max}$. Next, from all possible eigenvectors C_i that correspond to real quasimomenta k (a quasimomentum k is considered to be real if the imaginary part of the calculated kl is smaller than 10^{-10}), we choose only those for which the complex numbers $C_{in}^{\pm}$, with n in the vicinity of $n_{\min}$ and $n_{\max}$, are negligibly small [i.e., the probabilities $P_{\beta N}(k)$ defined below by Eq. (A29) are smaller than 10^{-10}]. It is found that for the intensities considered here, both for the band structure and the corresponding Floquet-Bloch states of the first three bands it suffices to assume that $n_{\max}=-n_{\min}=15$ to satisfy the above accuracy. We may note also that for the convergence to this accuracy the truncation size is very sensitive to the laser field intensity and increases very rapidly with increasing intensity.

Due to the time periodicity of the Schrödinger equation (A2) the quasienergy E is defined modulo ω. Therefore, we are free to choose any finite range of width ω in which the quasienergy changes continuously. In this paper we assume that E to be in the first Floquet zone, i.e., in the interval $[0,\omega)$. If one considers the quasienergy to be equal to, say, $E+n_0\omega$ with $E\in[0,\omega)$, then in order to find the corresponding Floquet-Bloch state it suffices to make the following substitutions in Eq. (A4) (e.g. [23]):

$$E\rightarrow E-n_0\omega \tag{A17}$$

and

$$C_{in}^{\pm}\rightarrow C_{i,n+n_0}^{\pm}. \tag{A18}$$

In other words, if we know the band structure and the Floquet-Bloch states for quasienergies from the interval $[0,\omega)$, then with the help of the above rules we can find them for any real E. From the computational point of view it is most convenient to take such values for the quasienergies that are near to the field-free energies of the physically relevant states. Otherwise, as follows from the above results, in order to find the relevant eigenstates one would have to consider a much larger truncation size than is necessary.

We now discuss another technical problem which arises due to the method of solution of the eigenvalue equation in which a set of k eigenvalues are generated for a chosen value of the energy E. It is necessary, in this circumstance, to have a way of ordering the pairs $(k,E(k))$ that belong to an energy ordered band characterized by, say, the index $\beta=1,2,3,\ldots$. In the absence of the field there is no special problem, but, in the presence of the field, due to the multivalued nature of the Floquet eigenvalues, this becomes a nontrivial technical problem. Below we shall first introduce the concept of the ''mean band energy,'' which, unlike the Floquet-Bloch eigenenergy, is independent of the choice of the Floquet zone. This invariant single-valued quantity is found to be most convenient not only for describing the physical properties of the system but also for resolving the band identification problem mentioned above. Let the Floquet-Bloch state with a band-ordering index β be written as

$$\psi_{\beta k}(x,t)=e^{-iE_\beta(k)t}\sum_{\sigma=\pm}\sum_{N,n\in\mathcal{Z}}e^{-iN(\omega t+\delta)}\times J_{N-n}(\sigma\alpha_0 p_{\beta in})e^{i\sigma p_{\beta in}x}C_{in}^{\beta\sigma},$$
$$x_{i-1}\leqslant x<x_i,\quad i=1,2,\ldots i_0 \tag{A19}$$

with

$$p_{\beta in}=\sqrt{2\mu[E_\beta(k)+n\omega-V_i]}. \tag{A20}$$

The probability density associated with this state is equal to

$$\rho_{\beta k}(x,t)=\sum_{m\in\mathcal{Z}}e^{-im(\omega t+\delta)}\rho_{\beta km}(x), \tag{A21}$$

with

$$\rho_{\beta km}(x)=\mathcal{N}_{\beta k}^{-1}\sum_{\sigma,\sigma'=\pm}\sum_{n,n'\in\mathcal{Z}}\frac{1}{l}\times e^{i(\sigma p_{\beta in}-\sigma' p^*_{\beta in'})x},$$
$$\times J_{n'-n+m}(\sigma\alpha_0 p_{\beta in}-\sigma'\alpha_0 p^*_{\beta in'})C_{in}^{\beta\sigma}(C_{in'}^{\beta\sigma'})^*,$$
$$x_{i-1}\leqslant x<x_i. \tag{A22}$$

We normalize our Floquet-Bloch state such that ($T=2\pi/\omega$ is the period of the laser field oscillations)

$$\frac{1}{T}\int_0^T\int_0^l dt\,dx\,\rho_{\beta k}(x,t)=1, \tag{A23}$$

thus the normalization constant

$$\mathcal{N}_{\beta k}=\sum_{i=1}^{i_0}\sum_{\sigma,\sigma'=\pm}\sum_{n,n'\in\mathcal{Z}}n_i(\sigma p_{\beta in}-\sigma' p^*_{\beta in'})\times J_{n'-n}(\sigma\alpha_0 p_{\beta in}-\sigma'\alpha_0 p^*_{\beta in'})C_{in}^{\beta\sigma}(C_{in'}^{\beta\sigma'})^*, \tag{A24}$$

where i_0 is defined by the space periodicity condition $x_{i+i_0}=x_i+l$, and for the Kronig-Penney-like potential, Eq. (23), considered in this paper $i_0=2$, and

$$n_i(y)=\frac{1}{l}\int_{x_{i-1}}^{x_i}dx\,e^{iyx}=\frac{e^{iyx_i}-e^{iyx_{i-1}}}{ily}. \tag{A25}$$

Let the time-dependent probability, Eq. (A21), integrated over an elementary cell, be

$$\rho_{\beta k}(t)=\sum_{m\in\mathcal{Z}}e^{-im(\omega t+\delta)}\rho_{\beta m}(k), \tag{A26}$$

with the Fourier components

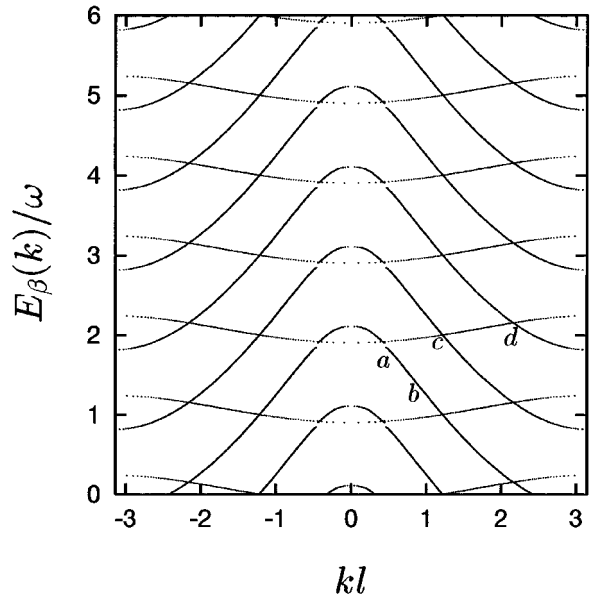

FIG. 15. The first two bands for the laser intensity $I=3.51\times10^{10}$ W/cm^2 and the photon energy $\omega=1.169$ eV. Notice that for this low intensity the tightly bound first band is hardly affected, whereas the second band changes qualitatively from the corresponding field-free case (cf. Fig. 2). A minigap (a) appears, which is due to the two-photon resonant coupling of the second band with the third. (b), (c), and (d) are in fact very narrow minigaps due to higher-order resonant couplings.

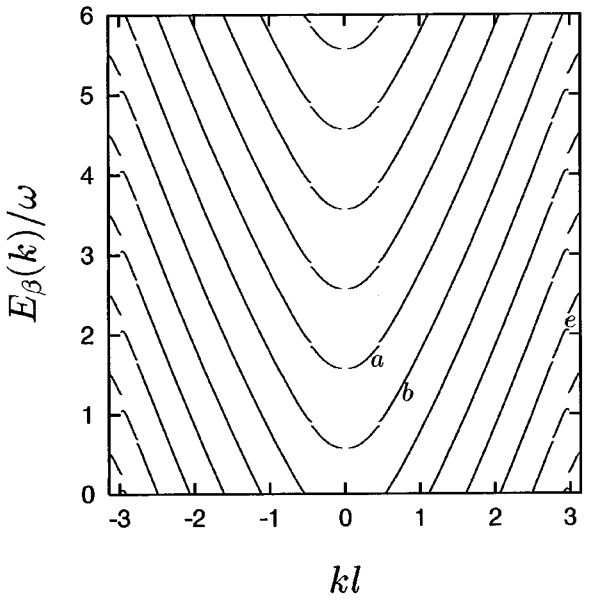

FIG. 16. This figure shows the third band at the laser intensity $I=3.51\times10^{10}$ W/cm^2 and $\omega=1.169$ eV. The minigap (e) is due to the one-photon resonant transition and the other minigaps (a) and (b) are due to two- or more-photon resonant transitions.

$$\rho_{\beta m}(k)=\mathcal{N}_{\beta k}^{-1}\sum_{i=1}^{i_0}\sum_{\sigma,\sigma'=\pm}\sum_{n,n'\in\mathcal{Z}} n_i(\sigma p_{\beta in}-\sigma' p^*_{\beta in'}) \times J_{n'-n+m}(\sigma\alpha_0 p_{\beta in}-\sigma'\alpha_0 p^*_{\beta in'}) \times C_{in}^{\beta\sigma}(C_{in'}^{\beta\sigma'})^*, \tag{A27}$$

and the normalization $\rho_{\beta 0}(k)=1$. Further we define a *mean energy* given by the time-averaged expectation value of the total Hamiltonian,

$$\mathcal{E}_\beta(k)=\frac{1}{T}\int_0^T\int_0^l dt\,dx\,\psi^*_{\beta k}(x,t)(\mathrm{i}\partial_t)\psi_{\beta k}(x,t)=\sum_{N\in\mathcal{Z}}(E_\beta(k)+N\omega)P_{\beta N}(k), \tag{A28}$$

with

$$P_{\beta N}(k)=\mathcal{N}_{\beta k}^{-1}\sum_{i=1}^{i_0}\sum_{\sigma,\sigma'=\pm}\sum_{n,n'\in\mathcal{Z}} n_i(\sigma p_{\beta in} -\sigma' p^*_{\beta in'})J_{N-n}(\sigma\alpha_0 p_{\beta in}) \times J_{N-n'}(\sigma'\alpha_0 p^*_{\beta in'})C_{in}^{\beta\sigma}(C_{in'}^{\beta\sigma'})^*. \tag{A29}$$

The usefulness of this quantity consists in the fact that for the field-free case the mean energy $\mathcal{E}_\beta(k)$ is exactly equal to the eigenenergy, and that in the presence of the field it is a ''structure quantity'' in the sense that it is independent of the choice of the Floquet zone chosen for the quasienergy. Since

$$\sum_{N\in\mathcal{Z}}P_{\beta N}(k)=1, \tag{A30}$$

therefore the real numbers $P_{\beta N}(k)$ can be interpreted as the probability, for a given k and β, of finding the electron with the energy $E_\beta(k)+N\omega$. With this interpretation the mean energy $\mathcal{E}_\beta(k)$ can be understood as the mean quasienergy given by the right-hand side of Eq. (A28),

$$\mathcal{E}_\beta(k)=\langle E_\beta(k)\rangle_{\beta k}. \tag{A31}$$

Moreover, we can define the *standard deviation* of the distribution of the electron energy in the photon space with a given k in band β,

$$\sigma_\beta(k)=\sqrt{\sum_{N\in\mathcal{Z}}[E_\beta(k)+N\omega]^2P_{\beta N}(k)-\langle E_\beta(k)\rangle^2_{\beta k}}, \tag{A32}$$

and the *band entropy*

$$S_\beta(k)=-\sum_{N\in\mathcal{Z}}P_{\beta N}(k)\ln(P_{\beta N}(k)). \tag{A33}$$

The standard deviation, or the band entropy, provides us with a measure of the fluctuations in the presence of the field of the electron energy associated with the band β and quasimomentum k. Clearly in the case of the vanishing radiation field, both $\sigma_\beta(k)$ and $S_\beta(k)$ are equal to zero.

The mean energies $\mathcal{E}_\beta(k)$ given by Eq. (A28) are plotted in Fig. 6 for three different intensities of the laser field. We see that far from the resonance peaks these plots are quite similar. This property suggests that we can use the mean energy spectrum to identify the actual band index β. Thus for the Kronig-Penney potential at the two intensities considered in the text ($I=10^{-6}$ and 10^{-5} a.u.), we identify

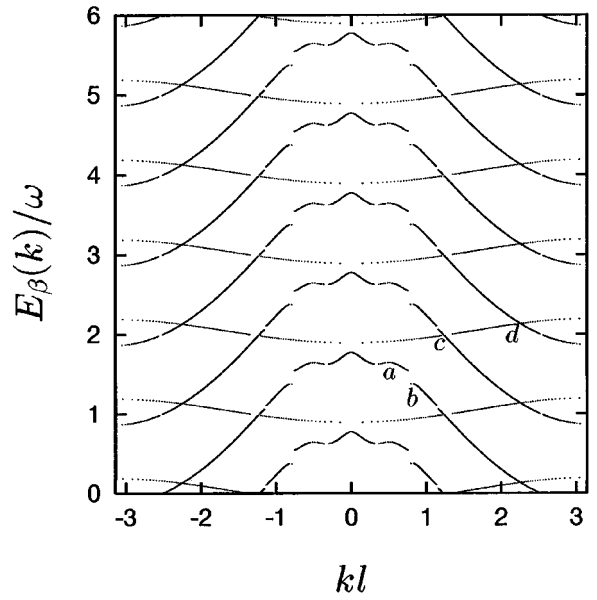

FIG. 17. The same as in Fig. 15, but for the larger intensity $I=3.51\times10^{11}$ W/cm^2. At this intensity the minigap (a), seen in Fig. 15, has completely disappeared, and the three-photon minigap (b) is significantly enlarged. The four- and five-photon minigaps (d) and (c), respectively, are not visible at the scale of the figure.

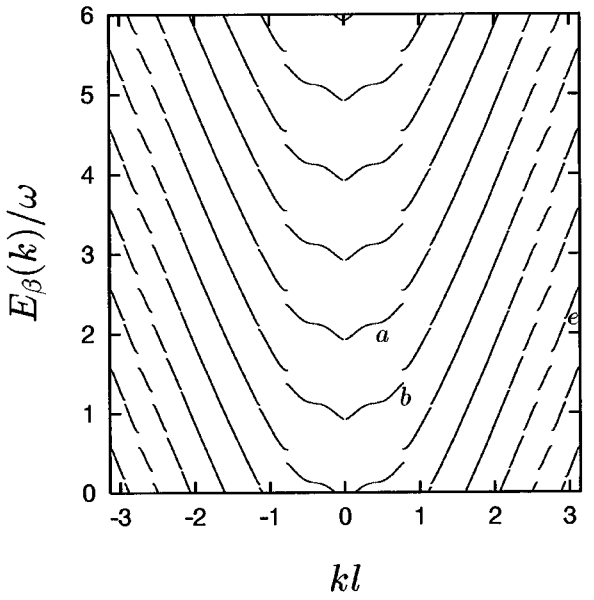

FIG. 18. The same as in Fig. 16, but for the larger intensity $I=3.51\times10^{11}$ W/cm^2.

$$\beta=\begin{cases}1, & \mathcal{E}_\beta(k)<-8.0\\ 2, & -8.0\leqslant\mathcal{E}_\beta(k)<-2.6,\\ 3, & -2.6\leqslant\mathcal{E}_\beta(k)<5.45\end{cases}\qquad\text{(A34)}$$

where the numerical values are in eV.

To associate the eigenvalues which appear in the (k,E) plane, with a given band index β we proceed as follows. We see from the unperturbed band structure, Fig. 2, that the first band lies at least between, say, $E_{1\min}=-12$ eV and $E_{1\max}=-8$ eV. Therefore, for all points in Figs. 4 or 5 we may associate only those for which the mean energy is larger than $E_{1\min}$ and smaller than $E_{1\max}$ to the first purturbed band $\beta=1$. Notice that this task was not difficult to carry out for both the intensities considered here, because the first band is greatly separated from the second band (by more than three times the photon energy). The association of the eigenvalues to the second band index is not as clear, since, although for a minimum energy we can take $E_{2\min}=-8$ eV, it is not obvious from Fig. 6 due to the proximity of the next band what the maximum energy $E_{2\max}$ must be. This difficulty, however, can be eliminated by requiring that the latter value must be unique for a given band, and that it must coincide with the quasienergies for a given quasimomentum k within modulo ω. This is fulfilled for $E_{2\max}=-2.6$ eV [34]. Applying the same procedure as for the second band, we found that the third band is determined by the mean energy between $E_{3\min}=-2.6$ eV and $E_{3\max}=5.45$ eV.

In Figs. 15–18 we present the identification of the Floquet-Bloch band structure in the presence of the field at $I=3.51\times10^{10}$ and 3.51×10^{11} W/cm^2 using the above labeling procedure.

[1] A. McPherson, G. Gibson, H. Jara, U. Johann, T. S. Luk, I. A. McIntyre, K. Boyer, and C. K. Rhodes, J. Opt. Soc. Am. **4**, 595 (1987); M. Ferray, A. L'Huillier, X. F. Li, L. A. Lompré, G. Mainfray, and C. Manus, J. Phys. B **21**, L31 (1988).

[2] G. Mainfray and C. Manus, Rep. Prog. Phys. **54**, 1333 (1991), and references therein.

[3] B. W. Shore and D. L. Knight, J. Phys. B **24** 325 (1987); T. H. Eberly, Q. Xu, and J. Javanainen, Phys. Rev. Lett. **62**, 881 (1989); F. H. M. Faisal, in *Atoms in Strong Fields*, edited by C. A. Nicolaides, C. W. Clark, and M. H. Nayfeh (Plenum, New York, 1990), pp. 407–424; J. L. Krause, K. J. Schafer, and K. C. Kulander, Phys. Rev. A **45**, 4998 (1992); K. C. Kulander, K. J. Schafer, and J. L. Krause, Phys. Rev. Lett. **68**, 3535 (1992); P. B. Corkum, *ibid.* **71**, 1994 (1993); M. Lewenstein, Ph. Balcou, M. Yu. Ivanov, A. L'Huillier, and P. B. Corkum, Phys. Rev. A **49**, 2117 (1994); W. Becker, S. Long, and J. K. McIver, *ibid.* **50**, 1540 (1994); P. Moreno, L. Plaja, and L. Roso, Europhys. Lett. **28**, 629 (1994); J. Peatross, M. V. Fedorov, and K. C. Kulander, J. Opt. Soc. Am. B **12**, 863 (1995); S. Long, W. Becker, and J. K. McIver, Phys. Rev. A **52**, 2209 (1995).

[4] Gy. Farkas, Cs. Tóth, S. D. Moustaizis, N. A. Papadogiannis, and C. Fotakis, Phys. Rev. A **46**, R3605 (1992), and references therein.

[5] For more recent experimental works about the high harmonic generation in solids, see D. von der Linde, T. Engers, G. Janke, P. Agostini, G. Grillon, E. Nibbering, A. Mysyrowicz, and A. Antonetti, Phys. Rev. A **52**, R25 (1995); S. Kohlweyer, G. D. Tsakiris, C.-G. Wahlström, C. Tillman, and I. Mercer, Opt. Commun. **117**, 431 (1995).

[6] L. Plaja and L. Roso-Franco, Phys. Rev. B **45**, 8334 (1992).
[7] S. Hüller and J. Meyer-ter-Vehn, Phys. Rev. A **48**, 3906 (1993).
[8] J. Z. Kamiński, J. Phys. C **6**, 1577 (1994).
[9] A. Misra and J. I. Gersten, Phys. Rev. B **43**, 1883 (1991); **45**, 8665 (1992); S. Varró and F. Ehlotzky, Phys. Rev. A **49**, 3106 (1994); J. Phys. B **28**, 121 (1995); P. Kálmán and T. Brabec, Phys. Rev. A **52**, R12 (1995).
[10] F. H. M. Faisal and J. Z. Kamiński, Phys. Rev. A **54**, R1769 (1996).
[11] J. G. Fujimoto, J. M. Liu, E. P. Ippen, and N. Bloembergen, Phys. Rev. Lett. **53**, 1837 (1984).
[12] R. L. Carman, D. W. Forslund, and J. M. Kindel, Phys. Rev. Lett. **46**, 29 (1981); R. L. Carman, C. K. Rhodes, and J. M. Benjamin, Phys. Rev. A **24**, 2649 (1981).
[13] A. Azouz, N. Stelmakh, J.-M. Lourtioz, D. Delacourt, D. Papillon, and J. Lehoux, Appl. Phys. Lett. **67**, 2263 (1995).
[14] L. E. Myers, D. D. Miller, R. C. Eckhardt, M. M. Fejer, and R. L. Byer, Opt. Lett. **20**, 52 (1995).
[15] C. J. van der Poel, J. D. Bierlein, J. B. Brown, and S. Cloak, Appl. Phys. Lett. **57**, 2074 (1990); J. D. Bierlien, D. B. Laubacher, J. B. Brown, and C. J. van der Poel, *ibid.* **56**, 1725 (1990).
[16] F. Bassani and G. P. Paravicini, *Electronic States and Optical Transitions in Solids* (Pergamon, Oxford, 1985).
[17] J. Callaway, *Quantum Theory of the Solid State*, 2nd ed. (Academic, Boston, 1991).
[18] See, e.g., *Science and Engineering of One- and Zero-Dimensional Semiconductors*, edited by S. P. Beaumont and C. M. S. Torres (Plenum, New York, 1990); *Physics of Quantum Electron Devices*, edited by F. Capasso (Springer, Berlin, 1990).
[19] R. de L. Kronig and W. G. Penney, Proc. R. Soc. London, Ser. A **130**, 499 (1931); see also, S. Flügge, *Practical Quantum Mechanics* (Springer, Berlin, 1971).
[20] N. Tsoar and J. I. Gersten, Phys. Rev. B **12**, 1132 (1978).
[21] F. H. M. Faisal and R. Genieser, Phys. Lett. A **141**, 297 (1989).
[22] F. H. M. Faisal, Radiat. Effects and Defects in Solids **122**, 27 (1991).
[23] F. H. M. Faisal, *Theory of Multiphoton Processes* (Plenum, New York, 1987).
[24] J. R. Taylor, *Scattering Theory* (Wiley, New York, 1972).
[25] L. Dimou and F. H. M. Faisal, Phys. Rev. Lett. **59**, 872 (1987).
[26] J. Z. Kamiński, Acta Phys. Pol. A **83**, 495 (1993).
[27] See, e.g., *Festkörper*, edited by W. Raith (Walter de Gruyter, Berlin, 1992), p. 221 for the work function W, and N. W. Ashcroft and N. D. Mermin, *Solid State Physics* (Holt, Rinehart and Winston, Philadelphia, 1976), p. 38, for the Fermi energy E_F.
[28] F. H. M. Faisal (unpublished).
[29] If the Fermi energy E_F is lower than the value for which the Floquet-Bloch states of both the first and the second bands are occupied, then the resonant process that moves an electron from the first occupied band to the second unoccupied band and back is allowed and the associated resonance is physically observable. A few of the resonances in these figures, however, are due to our use of the unsymmetrized wave function in the present investigation, which should be disregarded. Thus, for example, the resonance near $q=4$ in Figs. 11 and 12, which corresponds to the spurious transition from the second band to the fully occupied first band, is disregarded in our calculation of the power spectrum (cf. Figs. 13 and 14, below). For an alternative procedure of handling the spurious transitions see [6]. We note, however, that the most satisfactory procedure would be to fully antisymmetrize the many-electron wave function, which however remain prohibitive computationally.
[30] R. E. Peierls, *Quantum Theory of Solids* (Clarendon, Oxford, 1955); see the footnote on p. 79.
[31] J. Z. Kamiński, Z. Phys. D **16**, 153 (1990).
[32] S. Varró and F. Ehlotzky, J. Opt. Soc. Am. B **7**, 537 (1990); J. Z. Kamiński and F. Ehlotzky, Phys. Rev. A **50**, 4404 (1994).
[33] C. Jung and H. S. Taylor, Phys. Rev. A **23**, 1115 (1981); R. A. Sacks and A. Szöke, *ibid.* **40**, 5614 (1989).
[34] Note that had one chosen too small a value of $E_{2\max}$, one would have obtained a pseudogap in the quasimomenta k for which there is no quasienergy. Similarly with a choice of too large a value of $E_{2\max}$ one would obtain a quasimomentum for which there are more than one quasienergy, and hence prevent the choice of a unique value of β.